Non-perturbative Hydrostatic Equilibrium

J. Wisdom

August 5, 1996

Abstract

A non-perturbative treatment of hydrostatic equilibrium is presented. We find that the widely used third order Zharkov-Trubitsyn theory is not adequate to model the interiors of Jupiter and Saturn. We use the method to generate abstract objective interior models of the Jovian planets, with no input other than the observational data. The abstract objective models are in surprisingly good agreement with the physical models.

1 Introduction

Hydrostatic balance governs the basic shape of all planets. The physics is simple — in equilibrium the local pressure force must balance the gravitational and centrifugal forces. Material properties must be supplied to relate the density to the pressure.

The classical approach to the solution of the problem of hydrostatic balance is through perturbation theory. The perturbative treatments use various schemes to reduce the non-linear functional problem to a small set of coupled differential or integro-differential equations. The perturbation parameter is the ratio of the centrifugal acceleration to the gravitational acceleration at the surface at the equator. The classical perturbation theories find successive approximations to the level surfaces (surfaces of constant density and pressure) as functions of radius. Zharkov and Trubitsyn (1978) review modern extensions of the classical perturbation theories. Other approaches have been developed which are not based on level curves (e.g. Ostriker and Mark, 1968, Hubbard, Slattery, and DeVito, 1975). All recent models of the interiors of the Jovian planets have used the third order theory of Zharkov and Trubitsyn (1978) to solve the problem of hydrostatic balance (Podolak and Reynolds, 1987, Gudkova, et al., 1988, Hubbard and Marley, 1989, Chabrier, et al., 1992, Marley, et al., 1995, Hubbard, et al. 1995). We show below that the third-order Zharkov-Trubitsyn theory is not adequate to model the interiors of Jupiter and Saturn.

Computational resources are great enough today that many problems can be approached more simply and directly than was possible in earlier eras. In this computational era, we can focus attention on the basic physical processes, and use carefully crafted numerical methods to reliably determine the consequences of these physical

processes. The goals of this paper are twofold. First, it is to state completely and explicitly the problem of hydrostatic structure. Second, it is to present a straightforward computational solution to the simple problem of hydrostatic balance. The method of solution is inspired by the physical problem. Physically, the planet adjusts until surfaces of constant potential coincide with surfaces of constant density and pressure. Thus it is natural to organize the numerical solution around the level curves, and the numerical solution is found by letting the planet adjust itself. The method presented here is not perturbative in the usual sense, but of course representations by infinite series must be truncated, so there is an effective order. However, the method presented has no fundamental limitation. If more accuracy is needed the series can simply be extended.

In the presentation, we first state the problem precisely. Next we discuss possible representations of the solution. We then discuss methods of finding a solution, and construct a numerical implementation of the method. We test the method on a problem which can be solved by completely other means. Finally, we apply the method to a physical problem of interest – the determination of the interior structure of the Jovian planets.

2 Equations of Hydrostatic Balance

The basic equation of hydrostatic equilibrium is

$$\vec{\nabla} p = \rho \vec{g}, \tag{1}$$

where p is the pressure, ρ is the density, and $\vec{g}$ is the local acceleration, the gradient of the total potential,

$$\vec{g} = -\vec{\nabla} U. \tag{2}$$

The potential is the sum of the gravitational potential and the centrifugal potential. The gravitational potential is

$$U_G(\vec{r}) = -G \int \frac{\rho(\vec{r}\,')}{|\vec{r} - \vec{r}\,'|} d^3 r' \tag{3}$$

and the centrifugal potential is

$$U_R(\vec{r}) = -\frac{1}{2} \Omega^2 r_\perp^2 \tag{4}$$

where $r_\perp$ is the distance from the rotation axis.

We shall assume the pressure $p(\rho)$ is a function of density only (i.e. the interior is barotropic). Here we restrict attention to isolated rotating planets for which there are no significant external contributions to the potential. In this case, we expect the planet to be axisymmetric and possess north/south symmetry.

Through the equation of state $p(\rho)$ and the equation of hydrostatic equilibrium the density is directly related to the potential. For any radial line where the pressure

gradient and local acceleration are purely radial, such as a line in the equator plane or through the pole, the equation of hydrostatic equilibrium is a scalar differential equation

$$\frac{dp}{dr} = -\rho \frac{dU}{dr}. \tag{5}$$

The assumption that pressure is a function of density guarantees that surfaces of constant density correspond to surfaces of constant pressure, and the equation of hydrostatic balance then guarantees that surfaces of constant density and pressure are also surfaces of constant potential. We expect that all of these quantities vary monotonically from the center of the body to the surface of the body, and thus any of them can be expressed as a function of any of the others. The scalar equation of hydrostatic equilibrium can be formally integrated using density as the independent variable

$$\int_{\rho_0}^{\rho} \frac{1}{\rho} \frac{dp}{d\rho} d\rho = U(\rho_0) - U(\rho), \tag{6}$$

where ρ_0 refers to the density at some reference point such as the surface. That is, integration of the equation of state directly relates the density to the potential.

The problem is this: the density distribution gives rise to the potential, and the potential is related through the equation of state to the density. We seek a self consistent solution.

3 Level Surfaces

Surfaces of constant density, constant potential, and constant pressure coincide. The level surfaces are nested and can be labelled by a single continuous parameter s. It will be convenient to let s run from 0 at the center of the planet to 1 at the surface. We relate s to the radius of the level curve through

$$r(s, \mu) = Rs[1 + \eta(s, \mu)], \tag{7}$$

where μ is the cosine of the colatitude θ, and R is a characteristic radius of the planet. We shall refer to η as the "shape function." There is no dependence on the longitude because we have restricted our attention to axisymmetric planets. Further properties of the shape function must be specified to uniquely relate the parameter s to a particular level curve. For instance, we could specify that $\eta(1, 0) = 0$ so that R is the equatorial radius and Rs is the radius of the level curve on the equator plane. Alternatively, we could require that the volume enclosed by the level curve is the same as the volume enclosed by the sphere of radius Rs. However it is defined, a detailed representation for η must be chosen. Several possibilities come to mind: Chebyshev polynomials, Fourier series, Legendre polynomials. Each are complete, so any surface can be represented in terms of them. We postpone further specification of the shape function and its representation; subsequent development will guide our choices.

4 Development of the Potential

Given a distribution of mass, we need to know the potential at every point in the body. One approach is to just evaluate the appropriate integral over the mass distribution each time the potential is needed. Another approach is to express the potential in terms of moments of the mass distribution. Both approaches involve integrals of similar complexity. The latter approach is more attractive if the potential is approximated well by just a few moments, and will be evaluated at many places. We adopt this strategy.

Suppose we are interested in the potential on the level curve labelled by s. The potential on the level curve is the sum of the potential due to the mass inside the level curve and the potential of the mass outside the level curve. We shall label the region inside the level surface Region I, and the region outside the level surface but inside the planet as Region II. We determine the potential exterior to each of these regions as if there were no mass in the other region.

In a region in which there is no mass the potential satisfies Laplace's equation. The general axisymmetric solution of Laplace's equation is

$$U(r,\theta) = -\frac{GM}{R}\sum_{l=0}^{\infty}\left[c_l\left(\frac{r}{R}\right)^l + d_l\left(\frac{R}{r}\right)^{l+1}\right]P_l(\cos\theta), \tag{8}$$

where P_l are the usual Legendre polynomials, and c_l and d_l are free parameters. We have introduced scale factors so that the coefficients will be dimensionless. For potentials with north/south symmetry the sum is restricted to even l. The coefficients can be expressed as moments over the source mass distribution.

The potential in region I due to the mass in region II is

$$U_I(r,\theta) = -\frac{GM}{R}\sum_{l=0}^{\infty}c_{2l}\left(\frac{r}{R}\right)^{2l}P_{2l}(\cos\theta). \tag{9}$$

The terms with inverse powers of r are excluded because the potential is finite at the origin. The coefficients can be expressed as moments of the mass in region II:

$$c_l(s) = \frac{1}{M}\int_{II}\left(\frac{R}{r}\right)^{l+1}P_l(\cos\theta)\rho d^3r. \tag{10}$$

The potential in region II due to the mass in region I takes the form

$$U_{II}(r,\theta) = -\frac{GM}{R}\sum_{l=0}^{\infty}d_{2l}\left(\frac{R}{r}\right)^{2l+1}P_{2l}(\cos\theta). \tag{11}$$

The terms with positive powers of r are excluded because the potential is finite at infinity. The coefficients can be expressed as moments of the mass in region I:

$$d_l(s) = \frac{1}{M}\int_{I}\left(\frac{r}{R}\right)^{l}P_l(\cos\theta)\rho d^3r. \tag{12}$$

Note that all integrals are well defined and have finite values. Both solutions are valid at all points of the level surface of interest, the level surface that separates the two regions. The total potential is the sum of the two contributions.

We introduce a non-dimensional density ζ through $\rho = \bar{\rho}\zeta$, with $\bar{\rho} = M/(\frac{4}{3}\pi R^3)$, the mean density for a spherical planet of mass M and radius R. We reexpress the integrals for the dimensionless moments in terms of ζ and the level parameter s:

$$c_l(s') = 3\int_0^1 \left[\int_{s'}^1 \zeta(s)\frac{1}{s^{l-1}(1+\eta)^{l-1}}\left(1+\eta+s\frac{\partial\eta}{\partial s}\right)ds\right] P_l(\mu)d\mu \tag{13}$$

and

$$d_l(s') = 3\int_0^1 \left[\int_0^{s'} \zeta(s)s^{l+2}(1+\eta)^{l+2}\left(1+\eta+s\frac{\partial\eta}{\partial s}\right)ds\right] P_l(\mu)d\mu. \tag{14}$$

For convenience, we also introduce a non-dimensional potential $\widetilde{U}$ through $U = -(GM/R)\widetilde{U}$. A non-dimensional measure of the relative strength of the centrifugal force to the gravitational force is $q = (\Omega^2 R)/(GM/R^2) = \Omega^2 R^3/GM$. If R is not the equatorial radius R_e we also refer to $q_e = \Omega^2 R_e^3/GM$.

5 Method of Solution

Given the density and shape as a function of the level curve parameter s, we can determine the potential at any point in the body. For a self-consistent hydrostatic solution, the potential at a level curve will be related to the density there by the equation of state, and all points on the level curve will have the same potential. It is natural to find this self-consistent solution by successive refinement of a trial solution. One way to do this would be to define some measure of the extent to which a solution is not in hydrostatic equilibrium and then gradually adjust the parameters ("hill climb") until a satisfactory solution is found. We pursue a different, more "physical" approach to the solution of these non-linear equations.

We motivate the method through the consideration of tides. If we apply an external potential to a planet, a "tide" is raised (the planet is distorted), and the density changes (the planet is squeezed). Let's divide the external potential at the surface into an average part and a part with zero average. The average part modifies the radial pressure balance; the other part distorts the body. Let ΔU represent the oscillating part of the external potential. At the surface of the planet, the height of the tide is approximately

$$\Delta r = -h\frac{\Delta U}{g}, \tag{15}$$

where ΔU is the part of the perturbing potential with zero average over the surface, g is the surface gravitational acceleration, and h is the "displacement Love number." The displacement Love number is a measure of the responsiveness of the planet. For a fluid homogeneous incompressible planet $h = 5/2$. For a tenuous (massless)

atmosphere above a point mass core $h = 1$. We could generalize the displacement Love number to be a function of level surface $h(s)$. This function would tell us how responsive a level surface is to an applied potential perturbation.

We consider an iterative approach to the determination of the hydrostatic solution. We let the numerical planet adjust itself to find the equilibrium. More specifically, we presume we have some approximation to the solution, and we would like to improve it. From the approximate solution we can calculate a new estimate of the potential, and the problem is how to adjust the planet to be more self-consistent. Inspired by the discussion of the tides, we compute the potential on each level surface. We use the average of this potential to adjust the density on the level surface; we treat the oscillating part of the potential on the level surface as a tidal potential which distorts the level surface according to equation (15). We do not know $h(s)$, so we use a conservative value of $h(s) = 1$.

A constraint on the level curve and density adjustment is that the total mass of the planet has the correct value:

$$M = \int \rho d^3 r', \tag{16}$$

which implies, by equation (12),

$$d_0(1) = 1. \tag{17}$$

If the change in a level curve preserves the volume enclosed by the level curve, and if the density does not vary strongly, then the mass enclosed by the level curve will be approximately preserved. Thus shape changes in the level curves will approximately decouple from changes in density on the level curve. This suggests that we parameterize the level curve shapes in such a way that volume is preserved, at least approximately, as the shape parameters change. This is accomplished, to first order in the coefficients, if we use a spherical harmonic expansion to represent the shape. In the axisymmetric case considered here, we use an expansion in Legendre polynomials. So we choose

$$\eta(s, \mu) = \sum_{l>0}^{\infty} a_l(s) P_l(\mu) \tag{18}$$

as our representation of the shape of the level curves for fixed s. North/south symmetry restricts l to be even. Note that with this choice s is approximately the radius of the sphere with volume equal to the volume enclosed by the level curve. (For analytical development we might have wanted to define s to have precisely this property, as Lyapunov does, but for us that would introduce extra non-linear constraints. See Zharkov and Trubitsyn, 1978.) Of course, we will have to truncate the expansion for practical calculations. The representation of the coefficient functions $a_l(s)$ and the density function $\zeta(s)$ is still unspecified. At this point we choose Chebyshev polynomials, because they are easy to use and have nice approximation properties.

Once the mass moments are computed, we can use them to compute the potential anywhere on a level surface. We then expand the angular dependence of the potential

variation in terms of Legendre polynomials:

$$\Delta U(s,\mu) = \sum_{l=0}^{\infty} \Delta U_l(s) P_l(\mu), \tag{19}$$

where the disturbing potential coefficients are (even l only)

$$\Delta U_l(s) = (2l+1) \int_0^1 P_l(\mu) U(r(s,\mu),\mu) d\mu, \tag{20}$$

where $U(r,\mu)$ is expressed in terms of the moments, and $r(s,\mu)$ has the chosen representation. The ΔU_l for $l > 0$ are used to compute the adjustment to the level curve shapes through the the tidal distortion formula; ΔU_0 is used to adjust the density of level curve s. The radial functions are represented by Chebyshev interpolations, so the calculation is carried out for each of the Chebyshev interpolation points in s. The whole process is repeated until adequate convergence is achieved.

Here are some details of the implementation. We evaluate integrals using a rational extrapolation of the second Euler-Maclaurin formula, with interval divisions of 2, 3, 4, 6, 8, and 12. If the estimated relative error is unsatisfactory, the interval is divided into two equal parts and the process is applied recursively to the parts. Typically we require 10^{-11} relative accuracy of the quadratures, but the accuracy achieved is usually much better than this. This method is accurate and efficient, and works even when the integrand has singularities. Legendre polynomials are evaluated by forward recurrence; sums of Legendre polynomials are evaluated using the Clenshaw recurrence formula. Sums of Chebyshev polynomials are similarly evaluated with the Clenshaw recurrence. We found that for an $n = 1$ polytrope (see below) that the iteration is stable with $h(s) = 1$, but unstable if we use a more aggressive $h(s) = 5/2$. We did not try to determine an optimal h. Every few iterations we extrapolated the iterative solutions, using the Aitken-Steffenson method (see Danby, 1988). The method is applied point-wise to each of the radial functions at the Chebyshev interpolation points. Sometimes this dramatically improves the convergence.

6 Polytropes

A nice test case is a rotating planet with a polytropic equation of state. For a polytrope the pressure is related to the density by

$$p = C\rho^{\gamma}, \tag{21}$$

where $\gamma = 1 + 1/n$, with polytropic index n, and C is a constant. It happens that $n = 1$ is not a bad first approximation to the effective equation of state for the interior of Jupiter. A non-rotating polytrope with $n = 1$ can be solved analytically. A rotating polytrope with index $n = 1$ can be solved by other means, so we can check our answers by computing both solutions.

The potential is, according to equation (6),

$$U(\rho) - U(\rho_0) = -C\frac{\gamma}{\gamma - 1}\left(\rho^{\gamma-1} - \rho_0^{\gamma-1}\right). \tag{22}$$

A convenient choice for the reference point is the surface. For a polytrope the surface density is zero: $\rho_0 = 0$. For $n = 1$ we have

$$U(\rho) - U_0 = -2C\rho \tag{23}$$

We use this to adjust the density to be consistent with the potential.

Solutions for $n = 1$ have been found for a number of rotation parameters q. We present one in detail. In Figure 1 we show the radial functions for the "converged" solution for $q = 0.15$. In this solution we used 15 point Chebyshev interpolation for the radial functions, and terms up to $l = 10$ in the shape functions. Also shown are the differences between successive iterations. Note that these differences are quite small. We presume these small differences indicate that the solution has converged. The wiggles in the shape functions at small s for $l = 8$ and 10 are probably artifacts, but the cause is not obvious. As we shall see the solution is more than sufficient. The deduced value of the equatorial radius is $R_e = (1+\eta(1,0))R = 1.04432988740583R$. The effective perturbation parameter at this radius is $q_e = q(R_e/R)^3 = 0.17084582900350$. The derived gravitational moments are shown in the Table 1. We shall estimate the errors in this solution by finding an independent solution. The table also lists derived quantities for the other solutions, which are described below.

Table 1

	order 10	order 12	Bessel
R_e/R	1.0443298874	1.0443300982	1.0443301060
q_e	0.1708458290	0.1708459325	0.1708459363
J_2	0.0245154407	0.0245154308	0.0245154305
J_4	−.0016441385	−.0016441371	−.0016441371
J_6	0.0001649217	0.0001649213	0.0001649213
J_8	−.0000207333	−.0000207320	−.0000207319
J_{10}	0.0000030149	0.0000030107	0.0000030104
J_{12}	−.0000004764	−.0000004838	−.0000004829

7 Alternate Solution

A rotating polytrope with $n = 1$ can be solved independently by another method. The gravitational potential U_G interior to the body satisfies Poisson's equation

$$\nabla^2 U_G = 4\pi G\rho. \tag{24}$$

The rotational potential U_R satisfies

$$\nabla^2 U_R = -2\Omega^2. \tag{25}$$

Thus the total potential satisfies

$$\nabla^2 U = 4\pi G\rho - 2\Omega^2. \tag{26}$$

For an $n = 1$ polytrope, using equation (23), this becomes

$$\nabla^2 \rho + \frac{2\pi G}{C}\rho = \frac{\Omega^2}{C}. \tag{27}$$

We again introduce a non-dimensional density ζ through $\rho = \bar{\rho}\zeta$. Here ζ is a function of r and θ. We will not be finding or using level curves, but we will make use of a surface function:

$$r_s(\mu) = R(1 + \eta(\mu)). \tag{28}$$

We shall represent η in terms of Legendre polynomials

$$\eta(\mu) = \sum_{l>0}^{\infty} a_l P_l(\mu) \tag{29}$$

These definitions parallel those for the more general level surface approach, but here the coefficients are not functions of s. We can represent C with a non-dimensional parameter α through

$$C = \frac{1}{\alpha^2}\frac{2}{\pi}GR^2. \tag{30}$$

Scaling the spatial derivatives by R^2, we derive a non-dimensional version of equation (27)

$$\nabla^2 \zeta + \alpha^2\pi^2\zeta = \alpha^2\pi^2\frac{2q}{3}. \tag{31}$$

Let

$$\zeta' = \zeta - \frac{2q}{3}, \tag{32}$$

then ζ' satisfies the Helmholtz equation

$$\nabla^2 \zeta' + \alpha^2\pi^2\zeta' = 0. \tag{33}$$

The general axisymmetric solution of the Helmholtz equation is

$$\zeta'(r,\mu) = \sum_{l=0}^{\infty} b_l j_l(\alpha\pi r)P_l(\mu), \tag{34}$$

where b_l are constants to be determined, j_l are the usual spherical Bessel functions, P_l are the Legendre polynomials. The non-dimensional density is

$$\zeta(r,\mu) = \frac{2q}{3} + \sum_{l=0}^{\infty} b_l j_l(\alpha\pi r)P_l(\mu). \tag{35}$$

The surface is determined by $\zeta(1+\eta(\mu),\mu)=0$.

The problem is reduced to finding the set of coefficients b_l, and α, for which the solution is self-consistent. We can do this by adjusting the b_l until the surface is an equipotential. Our method for doing this is very similar to the method of solution for the other formulation. We compute the potential on the surface of the planet and let the planet adjust to this potential. In detail, the first step is to solve for a representation of the surface given some set of b_l. We use a method like Newton's method but approximate the derivative of the density with respect to the radius by b_0. We use an intermediate representation of the surface as a Chebyshev interpolation, so we solve for the surface at the Chebyshev interpolation points. We then compute the potential at the surface. We do this as before by computing the mass moments, but here we only need the surface moments d_l. The details of the quadrature are of course completely different. Here the variables of integration are r and μ, and the boundary is the computed surface. In our representation the first dimensionless moment must be $d_0=1$ in order for the total mass to be M. We adjust b_0 (which is responsible for most of the mass) so that this will better satisfied: $b_0'=b_0/d_0$. We then compute the projections of the surface potential onto the Legendre polynomials. We would like to let the surface adjust to ΔU_l using the tidal distortion formula (15). We can do this approximately by expanding the equation for the surface $\zeta(1+\eta(\mu),\mu)=0$ to first order in η and using the orthogonality of the Legendre polynomials to solve for the adjustment to b_l. We find $\Delta b_l \approx \Delta\widetilde{U}_l b_0/j_l(\alpha\pi)$. The value of α is determined by the requirement that the representation of the surface as Legendre polynomials has constant term 1, that is, $a_0=0$. We solve for α iteratively as we compute the Legendre polynomial expansion of the surface. The whole process is repeated until adequate convergence is obtained. Here convergence is judged by the magnitudes of $\Delta\widetilde{U}_l$.

We have solved for $q=0.15$ again in order to compare the two solutions. Here we take terms up to $l=14$, and use 20 point Chebyshev interpolation. The relative error of the integration quadratures was set to 10^{-10}. Convergence was declared when all $|\Delta\widetilde{U}_l|<10^{-14}$. For reference the solution coefficients are: $b_0=3.2639471725844178$, $b_2=-0.8766150340908836$, $b_4=0.1066132351677717$, $b_6=-0.0178053455205318$, $b_8=0.0061392876641078$, $b_{10}=-0.0062290924191637$, $b_{12}=-0.4092594755440963$, $b_{14}=-51.9771710398529760$. All other quantities are computable from these. Derived values for R_e, q_e, and the gravitational moments are given in Table 1. Comparing this solution to the solution determined by the more general level curve method, we find the relative error in the equatorial radius is about $\Delta R_e/R_e \approx 2\times10^{-7}$, with naturally a similar relative error in q_e. The relative errors in the moments are $\Delta J_2/J_2\approx 4\times10^{-7}$, $\Delta J_4/J_4\approx 8\times10^{-7}$, $\Delta J_6/J_6\approx 2\times10^{-6}$, $\Delta J_8/J_8\approx 6\times10^{-5}$, $\Delta J_{10}/J_{10}\approx 1\times10^{-3}$, $\Delta J_{12}/J_{12}\approx 1\times10^{-2}$. Evidently, the solutions are adequate for the forseeable future.

The main error probably results from using only terms up to $l=10$ in the general solution. We can check this by adding the $l=12$ terms. We have extended the general solution for $q=0.15$, adding one term in l. Figure 2 shows the radial functions and the

convergence errors. This time we used 15 point Chebyshev interpolation. The derived values of R_e, q_e, and the gravitational moments are listed in Table 1. Comparing this solution to the Bessel solution, we find now $\Delta R_e/R_e \approx 8 \times 10^{-9}$. The relative errors in the moments are $\Delta J_2/J_2 \approx 1 \times 10^{-8}$, $\Delta J_4/J_4 \approx 2 \times 10^{-8}$, $\Delta J_6/J_6 \approx 6 \times 10^{-9}$, $\Delta J_8/J_8 \approx 2 \times 10^{-6}$, $\Delta J_{10}/J_{10} \approx 1 \times 10^{-4}$, $\Delta J_{12}/J_{12} \approx 2 \times 10^{-3}$. Typically, extending the solution to $l = 12$ has reduced the errors in the derived quantities by one order of magnitude (more than a factor of q). Note also that the reduction of the order of the Chebyshev interpolation did not matter.

8 Comparison to Zharkov-Trubitsyn

Hubbard has kindly provided some solutions using the third order Zharkov-Trubitsyn theory for comparison (Hubbard, 1995). We have compared two particular cases. The first has a $q = 0.15896457$, near that of Saturn. The Zharkov-Trubitsyn third order theory gives $J_2 = 0.023108786$, $J_4 = -0.0014480848$, and $J_6 = 0.00012562161$. Using the bessel method, we find for $q = 0.1589645368308$, $J_2 = 0.0231048438421$, $J_4 = -0.0014589207833$, and $J_6 = 0.0001376974334$. Thus the errors in the Zharkov-Trubitsyn values are approximately $|\Delta J_2/J_2| \approx 2 \times 10^{-4}$, $|\Delta J_4/J_4| \approx 1\%$, and $|\Delta J_6/J_6| \approx 9\%$. The observational uncertainty in Saturn's J_6 is about 4% (see below). Thus the Zharkov-Trubitsyn theory is not adequate to model the interior of Saturn to observational accuracy. The large truncation error for Saturn's J_6 using the Zharkov-Trubitsyn third order theory was previously noted by Hubbard and Marley (1989). Indeed, their remark inspired the development of our more accurate method. The second test case has $q = 0.088570676$, for which the Zharkov-Trubitsyn moments are: $J_2 = 0.013905306$, $J_4 = -0.00052419360$, and $J_6 = 0.000028100375$. The bessel solutions, for $q = 0.0885706790713$, are $J_2 = 0.0139000788574$, $J_4 = -0.0005251005663$, $J_6 = 0.0000295470915$. The errors in the Zharkov-Trubitsyn values are thus approximately $|\Delta J_2/J_2| \approx 4 \times 10^{-4}$, $|\Delta J_4/J_4| \approx 0.002$, and $|\Delta J_6/J_6| \approx 5\%$. The observational uncertainty in Jupiter's J_2 is a part in $14,000$ (see below). Thus the Zharkov-Trubitsyn third order theory is not adequate to model Jupiter either.

9 Chebytropic Equations of State

The observables which provide the strongest constraints are the gravitational harmonics, and not many of these are known with great precision. The composition of the deep interior of the Jovian planets is unknown, and guesses based on surface composition or cosmogonic arguments are naturally uncertain. Thus interior models are poorly constrained physically. Even if the composition were known precisely, knowledge of the equation of state of complicated mixtures at high pressures and temperatures has its limitations. So typically a range of interior models are guessed that have a number of free parameters, and these parameters are determined by fitting the observational data. Adjustable parameters include: the mass and size of the

"rocky" core, helium mass fraction (which may vary in the planet due to varying solubilities), mass fraction of the non-hydrogen-helium component, perhaps specifically "ice" and "rock" fractions, parameters which express uncertainties in the equation of state, particularly in the metallic-molecular transition region, the temperature along the presumed adiabat, amount of differential rotation on cylinders or perhaps more general differential rotation, etc. One might wonder if the observational data are sufficient to address so many physical uncertainties in the models.

What happens if we throw out the uncertain interior physics entirely? Suppose instead we parametrize the effective equation of state abstractly, in such a way that we can add as many parameters as are well determined by the data, and no more. What will we get? Conventional wisdom is that the data do not provide sufficient constraints. We shall see.

In particular, we let the relation between density as a function of potential differences be represented as a polynomial. We use a parametrization of this polynomial as a sum of Chebyshev polynomials. In terms of non-dimensional potential $\widetilde{U}$ and non-dimensional density ζ, we choose

$$\zeta(\Delta\widetilde{U}) = \sum_{i=0}^{\infty} \zeta_i T_i(2\Delta\widetilde{U} - 1) \tag{36}$$

where $T_i(x)$ are the Chebyshev polynomials. The non-dimensional potential difference ranges roughly from 0 to 1; the shift and rescaling take the argument to roughly the range -1 to 1, which is the usual Chebyshev argument interval. We impose two restrictions on the expansion. First, we require that $\zeta(0)$ be the scaled surface density. Second, we require that $\zeta(\Delta\widetilde{U})$ be monotonic. This means that the density only increases as we go deeper into the planet. This is physically reasonable, but unfortunately does rule out interesting exotic planets with pure styrofoam cores. This assumption is required to maintain the interchangability of radius, pressure, density, and potential as independent variables that we have consistently assumed. Other than these constraints we let the data determine the rest. The order of the polynomial relating density to potential is extended until the observational data can be fit. Note that for an $n = 1$ polytrope, the density is linearly proportional to the potential difference, so an $n = 1$ polytrope is a member of the class of equations of state we are considering. From the determined polynomial $\zeta(\Delta\widetilde{U})$ we can compute the effective equation of state $P(\rho)$. We do this using the scalar equation of hydrostatic balance. Note that even though density is taken to be a polynomial function of potential, the pressure is not, in general, a polynomial function of density. We call our models "chebytropic" models, for obvious reasons.

10 Chebytropic Interiors of the Jovian Planets

We have found chebytropic interiors for Jupiter, Saturn, Uranus, and Neptune. The observational data which constrain these models consist of the mass, radius, gravitational harmonics. The observational data are presented in Table 2. Except for

Saturn, the data are the collection from Yoder (1994). For Saturn, values from Bosh (1994) are presented. The table also lists the observed flattening $f = (R_e - R_p)/R_e$, where R_e and R_p are the equatorial and polar radii.

Table 2

Planet	R_e	$J_2 \times 10^6$	$J_4 \times 10^6$	$J_6 \times 10^6$	$q_e \times 10^6$	f
Jupiter	71,492(4)	14,697(1)	−584(5)	31(20)	89,195(15)	0.06487(15)
Saturn	60,268(4)	16,335(6)	−898(9)	125(5)	154,815(31)	0.09796(18)
Uranus	25,559(4)	3,513(1)	−31.9(5)	???	29,535(48)	0.02293(8)
Neptune	24,766(15)	3,539(10)	−36(10)	???	26,085(57)	0.01710(140)

We use the downhill simplex method to adjust the chebytropic constants so as to minimize the sum of the squared differences between the model moments and the observed gravitational moments. For all the Jovian planets we take the surface density to be zero. The results are summarized in Table 3. The parameters for these chebytropic models are listed in the appendix. The number of digits presented is arbitrary and intentionally excessive.

Table 3

Planet	$J_2 \times 10^6$	$J_4 \times 10^6$	$J_6 \times 10^6$	$q_e \times 10^6$	C/MR_e^2	f
Jupiter	14,697.00	−581.69	33.95	89,196	0.2640	0.06489
Saturn	16,338.45	−897.56	78.33	154,819	0.2211	0.09644
Uranus	3,512.47	−32.49	0.46	29,535	0.2267	0.01983
Neptune	3,539.05	−33.04	0.46	26,085	0.2389	0.01819

For Jupiter we found we could fit the observational data with a cubic chebytrope. Presented in Figure 3 is a log-log plot of $P(\rho)$ for Jupiter. Plotted with the chebytropic model is a recent model from Hubbard (1995). The most striking aspect of the comparison is how well the abstract chebytrope does, particularly above a pressure of about a kilobar. Keep in mind that the chebytropic model was constructed without reference to any other model and without any input from high-pressure physics. There is no core in the chebytropic model (though there is a nod in that direction), and there is no hint of the discontinuity at the metallic phase transition (but the chebytrope goes smack thorough the middle). Neither is surprising because we have constrained the equation of state to be smooth. More disconcerting is that the chebytropic model does not agree with the physical model near the surface. At pressures less than a kilobar the pressure in the chebytropic model behaves approximately as $P = C\rho^2$. For a solar mixture of hydrogen and helium, the expected adiabatic law is $P = C\rho^{1.45}$. Apparently, the chebytropic model is inconsistent with the physics here, but on the other hand the gravitational moments are insensitive to the mass here. So the failure is not surprising. If we chop off the planet at a kilobar (which occurs at about

$s = 0.995$) then J_4 and J_6 are still within the observational error bounds. Interestly, significant contributions to J_2 continue to about the 150bar level (about $s = 0.998$). So the most sensitive indicator of density in the 150-1000bar range is J_2, not the higher moments. It is interesting that a core is not strongly indicated, or required to fit the observational data.

For Saturn, we were not able to fit all the observational data. However, we were able to find a fit for the data excluding J_6. Even in this case, we found we had to extend the chebytrope to sixth order in order to find a fit. (This is rather surprising, because we are only fitting three dimensionless observables: J_2, J_4, and q_e.) Presented in Figure 4 is a log-log plot of $P(\rho)$ for Saturn. Plotted with the chebytropic model is a recent model from Hubbard (1995). As for Jupiter, the deep interior is surprisingly well reproduced, but near the surface we have the same sort of discrepancy with the physics as we had with Jupiter. For Saturn, the nod in the direction of the core is stronger than it was for Jupiter.

For Uranus, the chebytrope was extended to a quintic before the observational data were fit. Presented in Figure 5 is a log-log plot of $P(\rho)$ for Uranus. The chebytropic model lies within the range of allowable physical models (see Podolak, Hubbard, and Stevenson, 1995). The most curious feature of the chebytropic fit is the *anti-core*: the slope of the $logP$ versus $log\rho$ line increases near the center of the planet. Indeed, lower order fits can be made for Uranus, but for them the density actually decreases near the core.

For Neptune, the chebytrope was also extended to a quintic before the observational data were fit. Presented in Figure 6 is a log-log plot of $P(\rho)$ for Neptune. The chebytropic model lies within the range of allowable physical models (see Podolak, Hubbard, and Stevenson, 1995).

In addition to the gravitational moments of the models, Table 3 lists the model flattening. Comparing the model values of the hydrostatic flattening to the observed flattening, we see that for Jupiter the model hydrostatic flattening is the same as the observed flattening within observational uncertainty. This is also true for Neptune, but the observational errors are large. The quoted observed value for Neptune is smaller than the hydrostatic value by about 6%. For Saturn and Uranus there is apparently a significant difference between the hydrostatic flattening and the observed flattening. For Saturn the hydrostatic flattening is too small by about 1%. For Uranus, the hydrostatic flattening is too small by a much larger percentage: about 14%.

Table 3 also lists the dimensionless polar moment of inertia $C/(MR_e^2)$, which is a key parameter in estimating the rate at which the spin axis of the planet precesses. For physical models of Jupiter and Saturn, Hubbard (1995) estimates the polar moments to be 0.264 and 0.220, respectively. These are in good agreement with the chebytropic values.

11 Conclusions

The principal contribution of this paper is a new method for the solution of hydrostatic balance which for all practical purposes has unlimited accuracy.

We find that the widely used Zharkov-Trubitsyn third order theory of hydrostatic balance is inadequate to generate quantitatively correct models of Jupiter and Saturn.

We have made interior models of the Jovian planets with an abstract polynomial equation of state. The minimal objective models agree surprisingly well with the parametrized physical models. Perhaps the agreement is indicative of actual model independent knowledge of the internal structure of the jovian planets.

12 Acknowledgements

We thank Bill Hubbard for extensive assistance in the comparison of our method and models to alternate methods and models, and also for many helpful discussions. We also thank Heidi Hammel, Phil Nicholson, Dave Stevenson, Chuck Yoder, and Maria Zuber for helpful discussions. We gratefully acknowledge support by the NASA Planetary Geology and Geophysics program under grant NAGW-706.

13 References

Bosh, A. (1994), MIT PhD Thesis.

Chabrier, G. Simon, D., Hubbard, W.B., Lunine, J. (1992), "The Molecular-Metallic Transition of Hydrogen and the Structure of Jupiter and Saturn" *Ap. J.* **391**, 817-826.

Guillot, T., Gautier, D., Chabrier, G., and Mosser, B. (1994), "Are the Giant Planets Fully Convective" *Icarus* **112**, 337-353.

Guillot, T., Chabrier, G., Morel, P., and Gautier, D. (1994), "Nonadiabatic Models of Jupiter and Saturn" *Icarus* **112**, 354-367.

Hubbard, W.B. (1984), *Planetary Interiors*, (Van Nostrand Reinhold, New York), p. 94.

Hubbard, W.B. (1995), personal communication.

Hubbard, W.B., and Marley, M.S. (1989), "Optimized Jupiter, Saturn, and Uranus Interior Models" *Icarus* **78**, 102-118.

Marley, M.S., Gomez, P. and Podolak, M. (1995), preprint.

Ostriker, J.P., and Mark, J.W-K. (1968), "Rapidly Rotating Stars. I. The Self Consistent Field Method" *Ap. J.* **151**, 1075-1087.

Yoder, C.F. (1994), "Astrometric and Geodetic Properties of Earth and the Solar System" in *Global Earth Physics: A Handbook of Physical Constants*, T. Ahrens, ed. (AGU, Washington, D.C.).

Zharkov, V.N., and Trubitsyn, V.P. (1978) *Physics of Planetary Interiors*, (Pachart, Tucson).

14 Appendix: Chebytrope Parameters for the Jovian Planets

This table lists the parameters of the best fit chebytropic models of the Jovian planets. Note that ζ_0 is determined from the other ζ_i by the requirement that the density at the surface is zero.

	Jupiter	*Saturn*	*Uranus*	*Neptune*
q	0.083246497685	0.139072479439	0.028943907223	0.025606667820
ζ_1	1.721229703723	2.081821959780	1.744632103786	1.723928752104
ζ_2	0.037400213201	0.383533477488	−.097198653912	−.045331478444
ζ_3	0.041258708992	0.104098145430	−.171938318090	−.052087981809
ζ_4	0	−.008892248292	0.050782411054	0.044640882430
ζ_5	0	−.011514183459	0.006482457479	−.033275955543
ζ_6	0	.000322077922	0	0

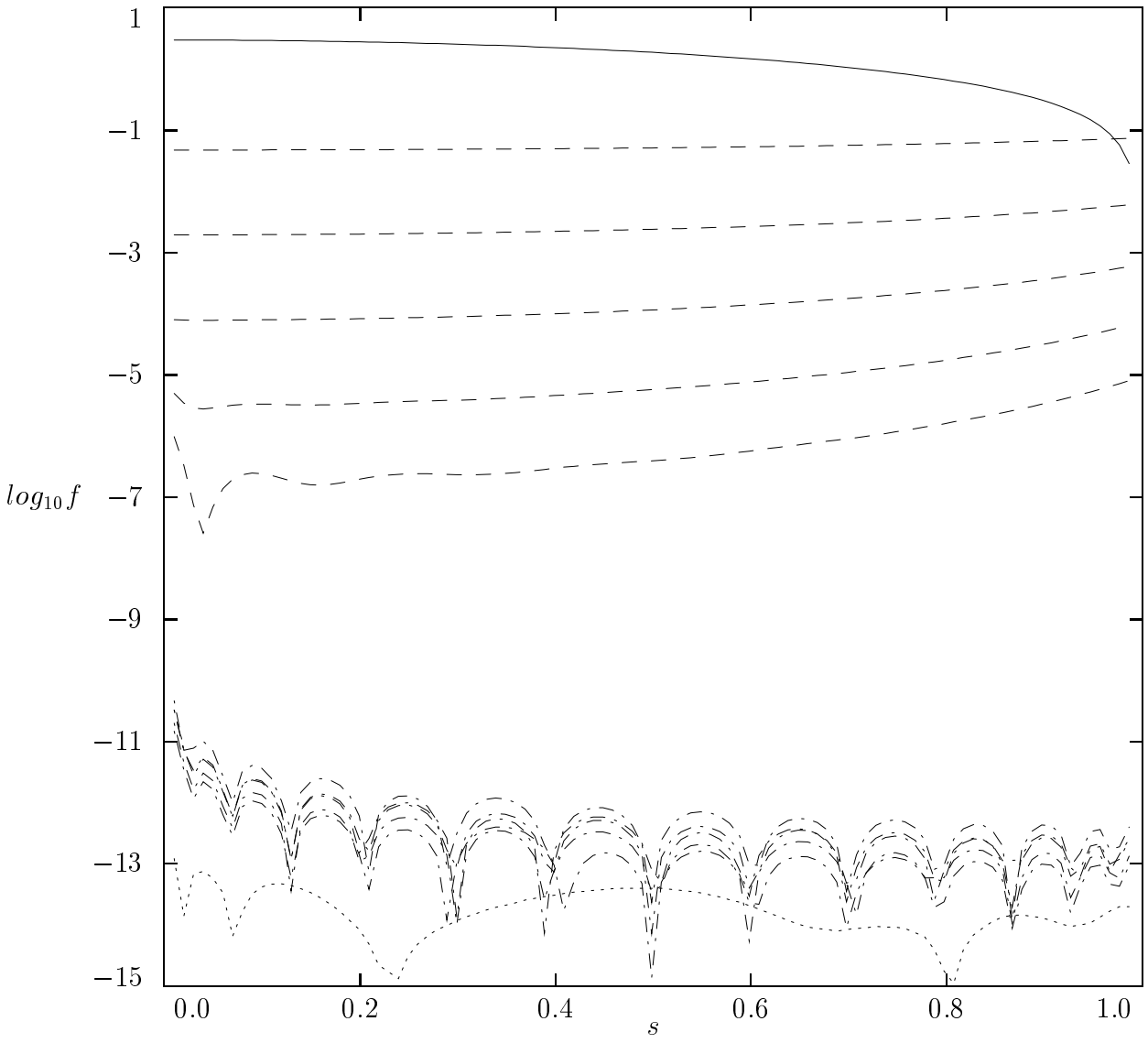

Figure 1: Radial functions for $q = 0.15$. The common logarithm of each function is plotted. The solid line is the non-dimensional density $\zeta(s)$. The dashed lines are the shape functions $a_l(s)$, for $l = 2, \ldots, 10$. Also shown are the differences between radial functions for two successive iterations. The dotted line is for the density, and the dot-dashed lines are for the shape functions.

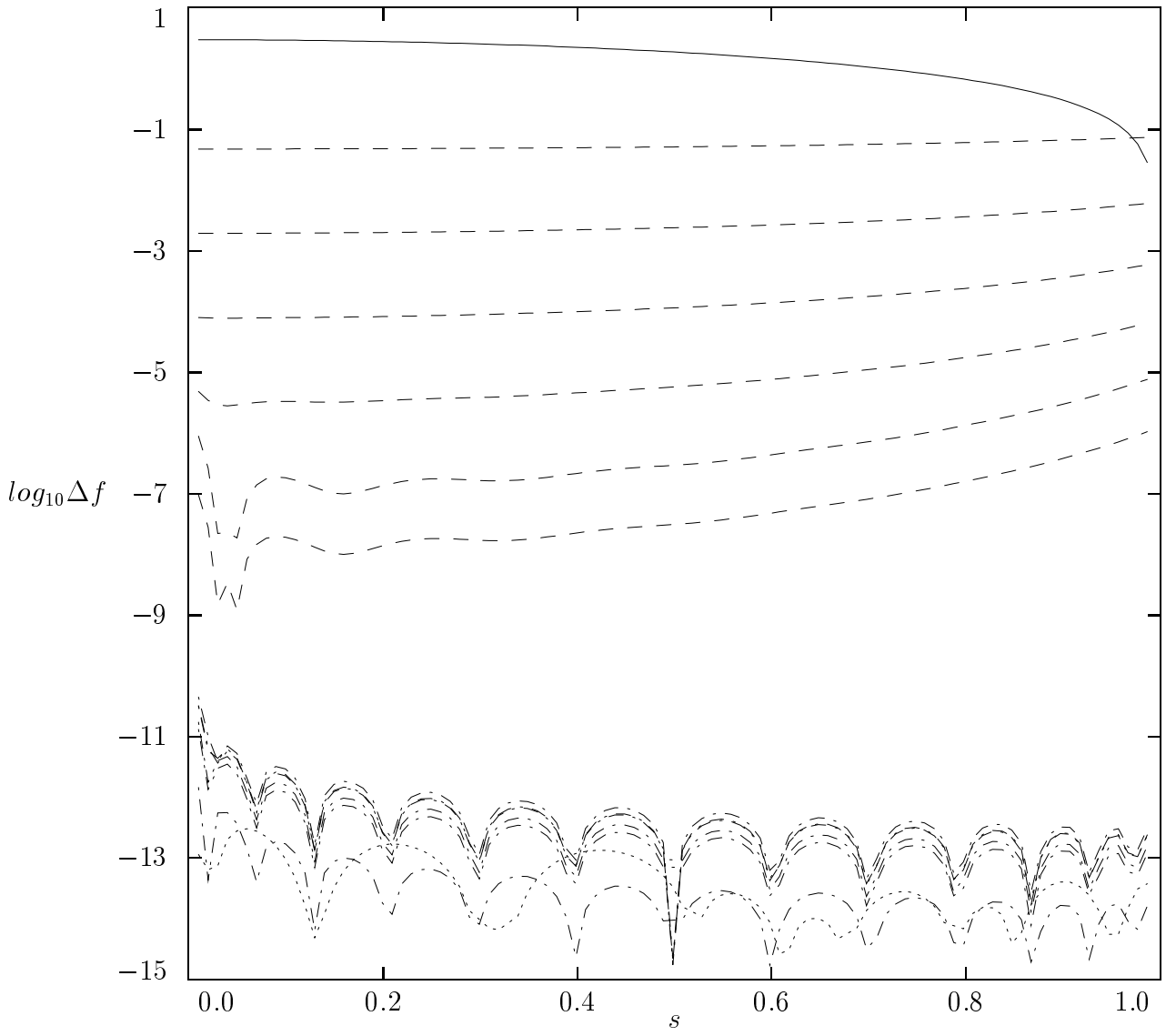

Figure 2: Radial functions for $q = 0.15$, extended to $l = 12$. The common logarithm of the function is plotted. The solid line is the non-dimensional density $\zeta(s)$. The dashed lines are the shape functions $a_l(s)$, for $l = 2, \ldots, 12$. Also shown are the differences between radial functions for two successive iterations. The dotted line is for the density, and the dot-dashed lines are for the shape functions.

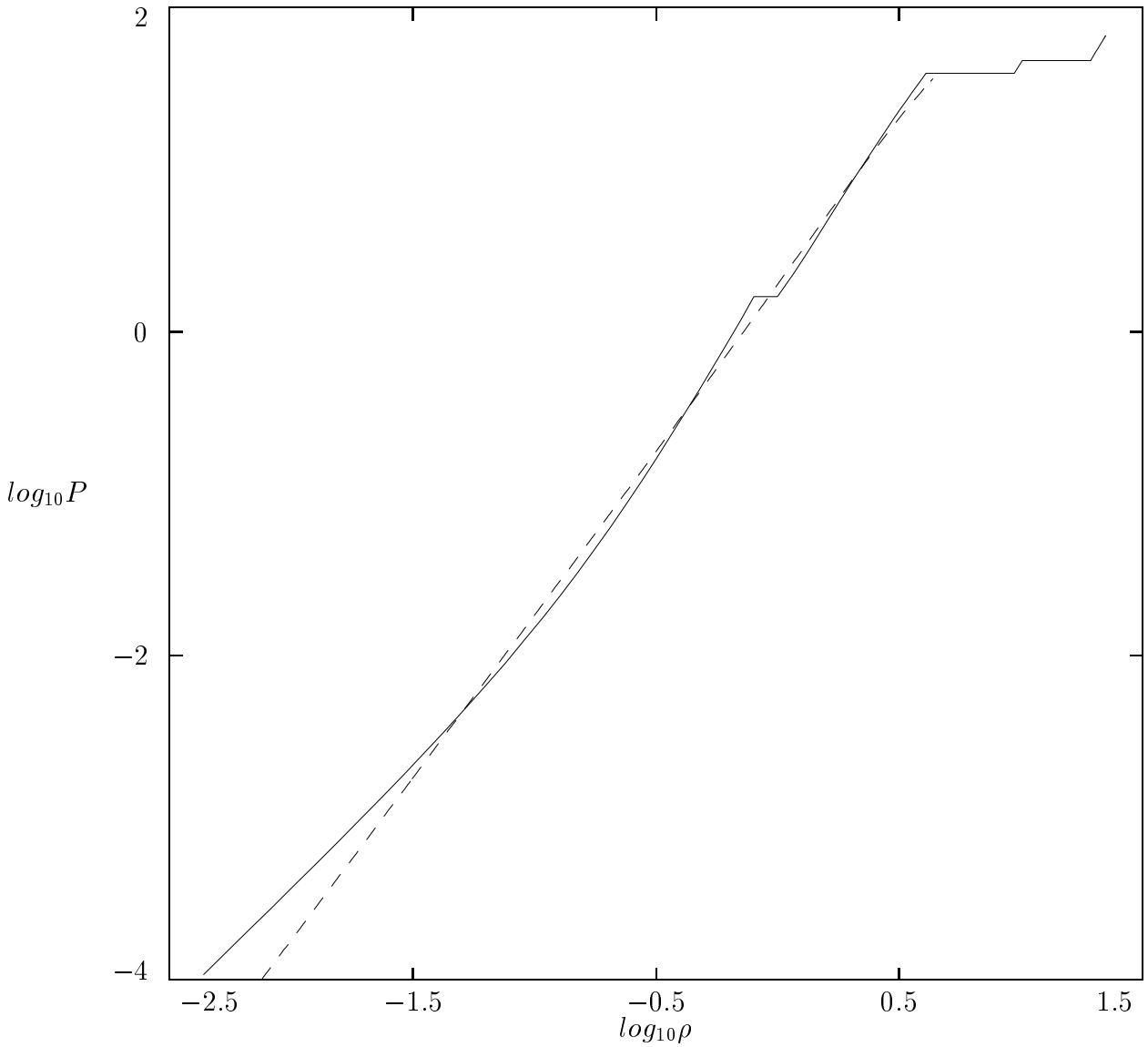

Figure 3: Pressure (in megabars) versus density (in g/cm^3) for Jupiter. The dashed line is for the chebytropic model. The solid line is a recent model from Hubbard (1995).

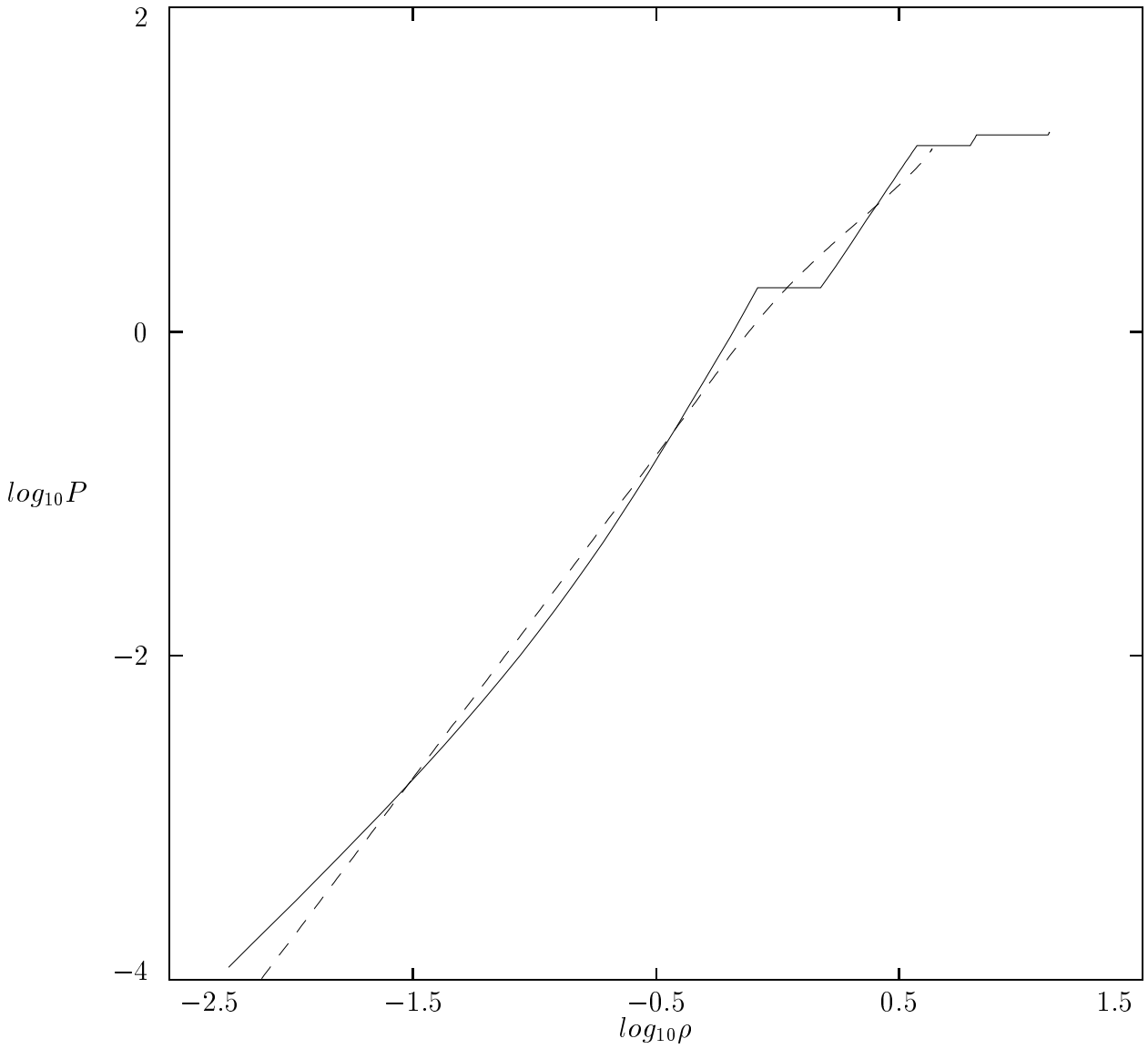

Figure 4: Pressure (in megabars) versus density (in g/cm^3) for Saturn. The dashed line is for the chebytropic model. The solid line is a recent model from Hubbard (1995).

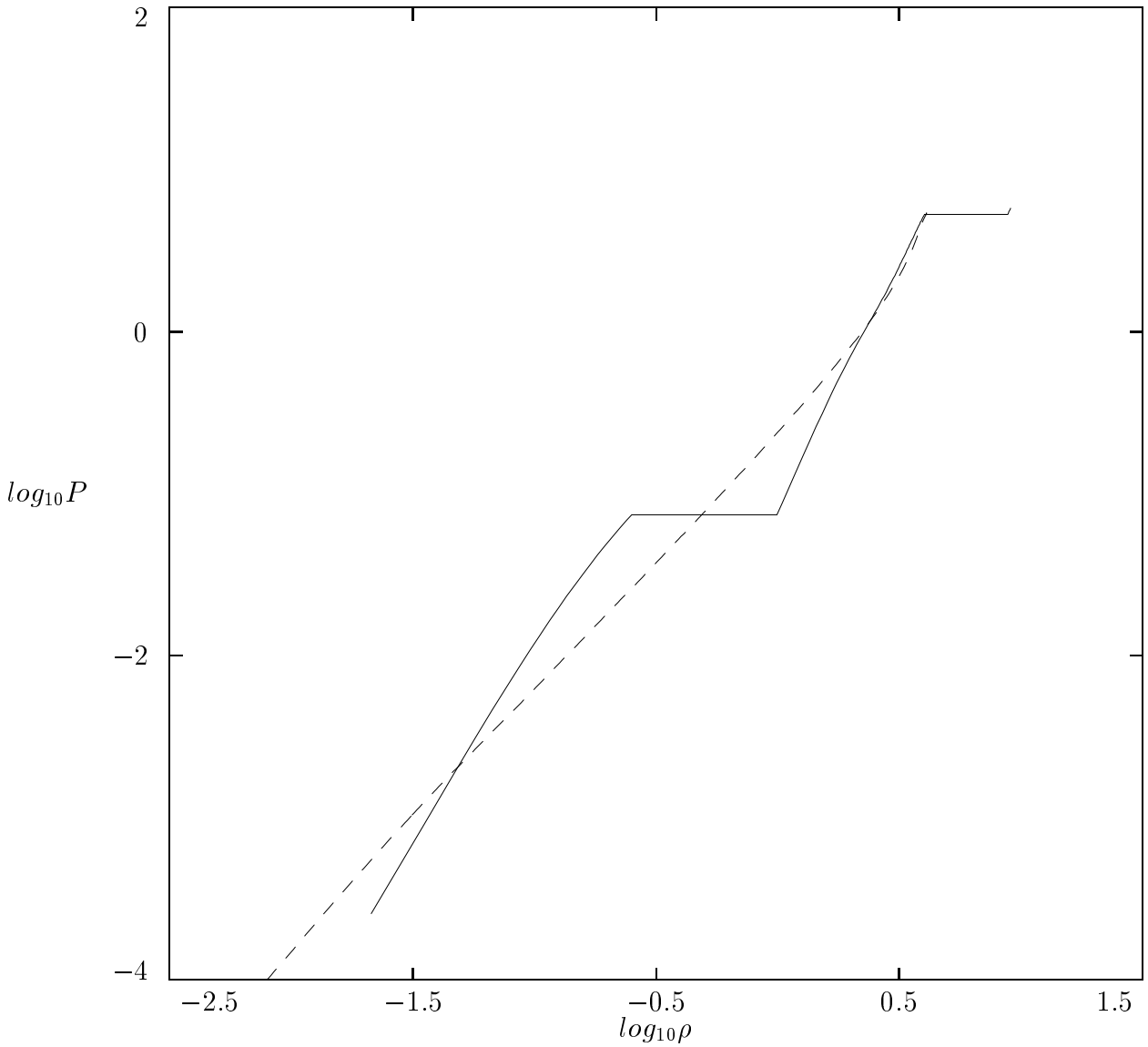

Figure 5: Pressure (in megabars) versus density (in g/cm^3) for Uranus. The dashed line is for the chebytropic model. The solid line is a recent model from Hubbard (1995).

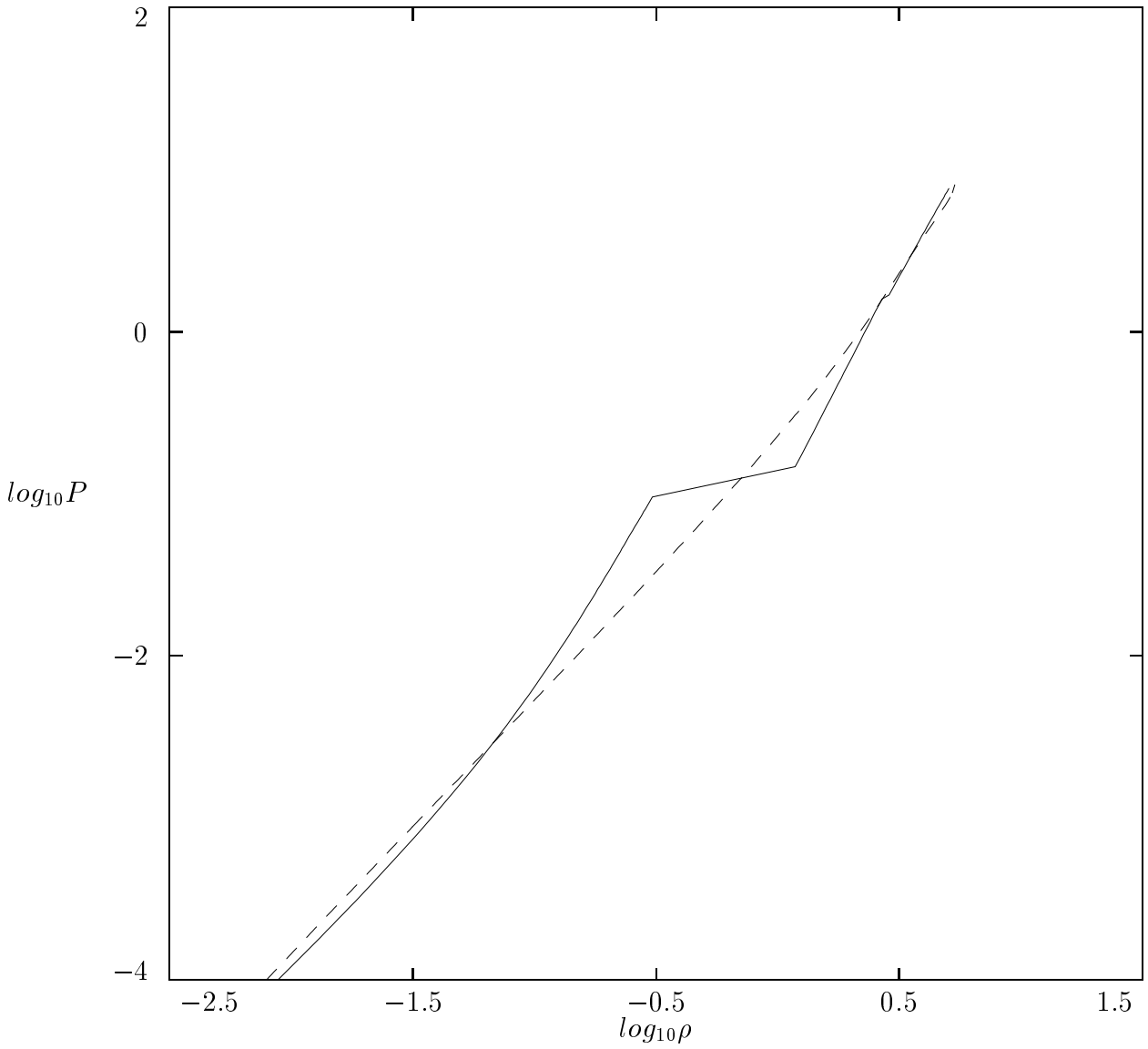

Figure 6: Pressure (in megabars) versus density (in g/cm^3) for Neptune. The dashed line is for the chebytropic model. The solid line is a recent model frmo Hubbard (1995).